We are IntechOpen, the world's leading publisher of Open Access books Built by scientists, for scientists

6,900
Open access books available

186,000
International authors and editors

200M
Downloads

Our authors are among the

154
Countries delivered to

TOP 1%
most cited scientists

12.2%
Contributors from top 500 universities

WEB OF SCIENCE™

Selection of our books indexed in the Book Citation Index in Web of Science™ Core Collection (BKCI)

Interested in publishing with us?
Contact book.department@intechopen.com

Numbers displayed above are based on latest data collected.
For more information visit www.intechopen.com

7

Pattern Effect Mitigation Technique using Optical Filters for Semiconductor-Optical-Amplifier based Wavelength Conversion

Jin Wang
Fraunhofer Institute for Telecommunications, Heinrich-Hertz-Institute
Germany

1. Introduction

The demand for bandwidth in telecommunication network has been increasing significantly in the last few years. It is to be expected that also in the next few years multimedia services will further increase the bandwidth requirement. To utilize the full bandwidth of the optical fibre, wavelength division multiplexing (WDM) and time-division multiplexing (TDM) techniques have been applied. In these two primary techniques, wavelength converters that translate optical signal of one wavelength into optical signals of another wavelength, see Fig. 1, have become key devices. In general, a wavelength converter has to be efficient, meaning that with low signal powers an error free converted signal can be obtained. Also, the wavelength converters have to be small, compact, and as simple (cheap) as possible.

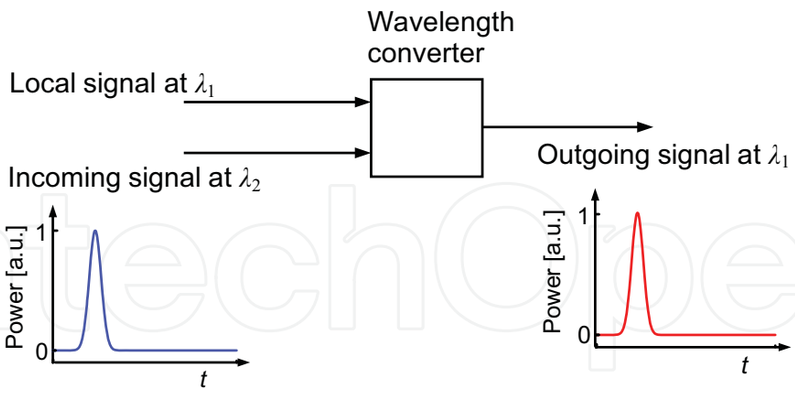

Fig. 1. A wavelength converter translates the incoming signal at λ_2 to the local signal at λ_1

Presently, large footprint optical-electrical-optical (o-e-o) translator units with large power consumption are used to perform wavelength conversion in optical cross-connects. Advantages of o-e-o methods are their inherent 3R (re-amplification, re-shaping, re-timing) regenerative capabilities and maturity. Conversely, the promise of all-optical wavelength conversion is the scalability to very high bit rates. All-optical wavelength converters (AOWC) can overcome wavelength blocking issues in next generation transparent networks and make possible reuse of the local wavelengths. All-optical wavelength converters can

also enable flexible routing and switching in the global and local networks, e.g. optical circuit-switching, optical burst-switching and optical packet-switching (Yoo, 1996).

Semiconductor optical amplifiers (SOAs) are closest to practical realization of all-optical wavelength converters (Yoo, 1996; Durhuus et al., 1996). SOA-based all-optical wavelength converters are compact, have low power consumption, and can be possibly operated at high speed. Indeed, a 320 Gbit/s SOA-based all-optical wavelength conversion has already been demonstrated (Liu et al., 2007). The advantages of using SOAs arise from the large number of stimulated emitted photons and free carriers, which are confined in a small active volume.

The SOA-based wavelength conversion works mostly via the variation of the gain and refractive index induced by an optical signal in the active region. The optical signal incident into the active region modifies the free carrier concentration. Thus, the optical gain and the refractive index within the active region are modulated. Other optical signals propagating simultaneously through the SOA also see these modulations of the gain and refractive index, being known as cross-gain modulation (XGM) and cross-phase modulation (XPM) (Yoo, 1996; Durhuus et al., 1996; Connelly, 2002). Thus, the information is transferred to another wavelength. In SOAs, a rich variety of dynamic processes drive the operation. These processes include the carrier dynamics between conduction band and valence band (interband dynamics) as well as inside of conduction band or valence band (intraband dynamics) (Connelly, 2002). They both affect the gain and the refractive index of the SOA, and thus the operation of the SOA-based wavelength converter. In addition, the fact that each of these effects has a specific lifetime leads to pattern dependent effects in the processed signals.

The pattern effect in the output signal out of an SOA is understood as follows. As subsequent incoming pulses are launched into a slow SOA, the carrier density is depleted continually. It recovers back to different levels and the amplifier gain also varies for different pulses, depending on the former bit pattern seen by the SOA. The unwanted pattern effect limits the implementation of the SOA-based wavelength converter at high speed.

The most practical approach to overcome pattern effects is to decrease the SOA recovery time by proper design (Zhang et al., 2006), optimum operation conditions (Girardin et al., 1998), an additional assisting light (Manning et al., 1994), and choice of new fast materials (Sugawara et al., 2002). Other approaches to mitigate the pattern effects are cascading several SOAs (Bischoff et al., 2004; Manning et al., 2006) or by using SOAs in a differential interferometer arrangement. Among them, the differential Mach-Zehnder interferometer (MZI) (Tajima, 1993), the differential Sagnac loop (Eiselt et al., 1995), the ultrafast nonlinear interferometer (UNI) (Hall & Rauschenbach, 1998) and the delay interferometer (DI) configurations (Leuthold et al., 2000), which exploit the XPM effect enable speeds beyond the limit due to the SOA carrier recovery times.

Recently, a new wavelength converter with an SOA followed by a single pulse reformatting optical filter (PROF) has been introduced (Leuthold et al., 2004b). In (Leuthold et al., 2004b), an experiment implementing a PROF based on MEMS technology demonstrated wavelength conversion at 40 Gbit/s, with record low input data signal powers of –8.5 and –17.5dBm for non-inverted and inverted operation. This is almost two orders of magnitudes less than typically reported for 40 Gbit/s wavelength conversions. The reason for the good conversion efficiency lies in the design of the filter. The PROF scheme exploits the fast chirp effects in the converted signal after the SOA and uses both the red- and blue-shifted spectral

components, while schemes with a single red- or blue-shifted filter (Leuthold et al., 2003; Nielsen & Mørk, 2006; Kumar et al., 2006; Liu et al., 2007) reject part of the spectrum. From an information technological point of view, rejection of spectral components with information should be avoided. Indeed, this scheme provides the best possible conversion efficiency for an SOA-based wavelength converter or regenerator.
The PROF scheme basically represents an optimum filter for the SOA response with the potential for highest speed operation. However, so far it is not clear, if these schemes with optical filters can successfully overcome pattern effects at highest speed.
In this chapter, we will show that the PROF scheme indeed and effectively mitigates SOA pattern effect. The pattern effect mitigation technique demonstrated here is based on the fact that the red chirp (decreasing frequency) and the blue chirp (increasing frequency) in the inverted signal behind an SOA have complementary pattern effects. If the two spectral components are superimposed by means of the PROF, then pattern effects can be successfully suppressed. An experimental implementation at 40 Gbit/s shows a signal quality factor improvement of 7.9 dB and 4.8 dB if compared to a blue- or red-shifted optical filter assisted wavelength converter scheme, respectively.
This chapter is organized as follows: In Section 2, an introduction of the SOA will be given. The basic SOA nonlinearities, which are used for wavelength conversion, will be reviewed. Also, the pattern effect in the SOA-based wavelength conversion will be discussed. In Section 3, the scheme of the SOA-based wavelength conversion assisted by an optical filter will be presented. The operation principle and experiment of this pattern effect mitigation technique are then explained and demonstrated.

2. Semiconductor-optical-amplifier based wavelength conversion

2.1 Semiconductor-optical-amplifier

Semiconductor-optical-amplifiers (SOAs) are amplifiers which use a semiconductor as the gain medium. These amplifiers have a similar structure to Fabry-Perot laser diodes but with anti-reflection elements at the end faces. SOAs are typically made from group III-V compound direct bandgap semiconductors such as GaAs/AlGaAs, InP/InGaAs, InP/InGaAsP and InP/InAlGaAs. Such amplifiers are often used in telecommunication systems in the form of fiber-pigtailed components, operating at signal wavelengths between 0.85 μm and 1.6 μm. SOAs are potentially less expensive than erbium doped fibre amplifier (EDFA) and can be integrated with semiconductor lasers, modulators, etc. However, the drawbacks of SOAs are challenging polarization dependences and a higher noise figure. Practically, the polarization dependence in the SOA can be reduced by an optimum structural design (Saitoh & Mukai, 1989).
A schematic diagram of a heterostructure SOA is given in Fig. 2. The active region, imparting gain to the input signal, is buried between the p- and n-doped layers, while the length of the active region is L. An external electrical current injects charge carriers into the active region and provides a gain to the optical input signal. An SOA typically has an amplifier gain of up to 30 dB.
Semiconductor amplifiers interact with the light, i.e. photons, in terms of electronic transitions. The transition between a high energy level W_2 in the conduction band (CB) and a lower energy level W_1 in the valence band (VB) can be radiative by emission of a photon with energy $hf = W_2 - W_1$ (h: Planck's constant, f: frequency), or non-radiative (such as thermal vibrations of the crystal lattice, Auger recombination). Three types of transitions,

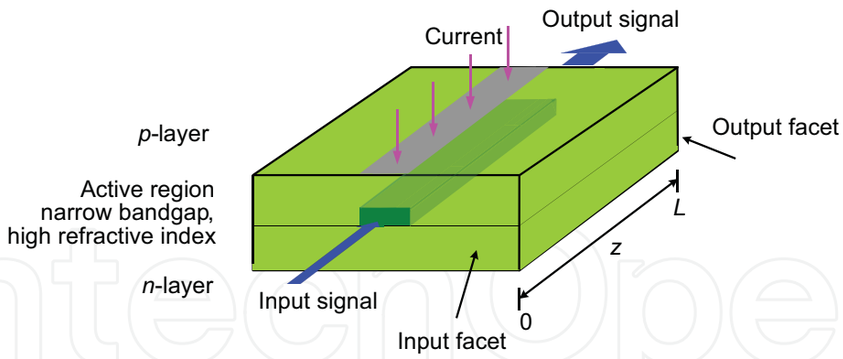

Fig. 2. Schematic diagram of an SOA

namely stimulated absorption, spontaneous emission and stimulated emission, are the basic mechanisms for all lasers and optical amplifiers. They are:

- Stimulated absorption: If an electromagnetic field exists, a photon with energy $hf = W_2 - W_1$ can be absorbed. Meanwhile, an electron can make an upwards transition from the lower energy level W_1 to the higher energy level W_2. The stimulated absorption rate depends on the electromagnetic energy density, and on the number of the electrons in the CB and the number of holes in the VB.
- Spontaneous emission: An electron in the CB can with a certain probability undergo a transition to the lower energy level W1 spontaneously, while emitting a photon with energy $hf = W_2 - W_1$, or loosing the transition energy through phonons or collisions. Obviously, the probability of the spontaneous emission is dependent on the number of the electron and hole pairs. These "spontaneously" emitted photons will be found with equal probability in any possible modes of the electromagnetic field. Thus a spontaneously emitted photon is regarded as a noise signal, since it represents a field with a random phase and a random direction.
- Stimulated emission: An incident photon can also induce with a certain probability a transition of the electron from the high energy level W_2 to the low energy level W_1. In this process a second photon is created. In contrast to spontaneous emission processes, this second photon is identical in all respects to the inducing photon (identical phase, frequency and direction). As does the stimulated absorption, the stimulated emission rate also depends on the incident electromagnetic energy density.

2.2 Basic SOA nonlinearities used for wavelength conversion

The SOA shows high nonlinearity with fast transient time. However, the high nonlinearity in the SOA is also accompanied with phase changes, which can distort the signals. This nonlinearity presents a most severe problem for optical communication applications, if the SOAs are used as "linear" optical amplifiers. Yet, high optical nonlinearity makes SOAs attractive for all-optical signal processing like all-optical switching and wavelength conversion. Indeed, the nonlinear gain and phase effects in an SOA, usually termed as cross-gain modulation (XGM) and cross-phase modulation (XPM), are widely used to perform wavelength conversion.

The XGM and XPM effects in an SOA are schematically shown in Fig. 3.

- XGM: As a strong control signal is launched into an SOA, it depletes the carrier in-side the SOA and saturates the gain of the SOA. If a weak probe signal (usually at a new

wavelength) is also present in the SOA, the amplification of the probe signal is affected by the strong control signal, see the output power in Fig. 3. Thereby, the probe signal is modulated by the control signal. This effect is called cross-gain modulation (XGM).

- XPM: As the control signal causes a change of the carrier density inside the SOA, it also induces a change of the refractive index and a phase shift of the probe signal when passing through the SOA, see the output phase in Fig. 3. This effect is called cross-phase modulation (XPM). The XPM effect is usually measured in an interferometric configuration.

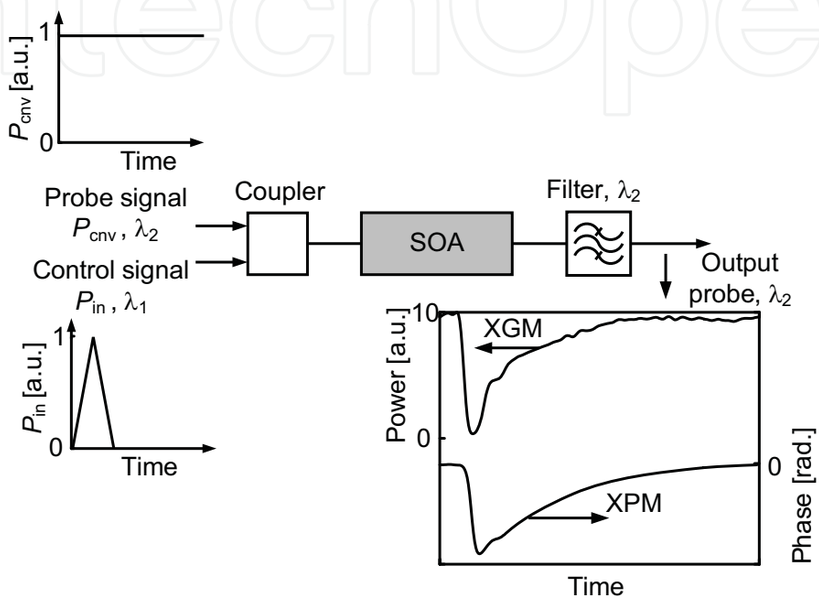

Fig. 3. XGM and XPM effects in an SOA. As an optical pulse of the input control signal at λ_1 is launched in the SOA, XGM and XPM effects are visualized by a cw probe signal at λ_2 at the output of the SOA, see left and right y-axes of the output signal.

In an SOA, the XGM and XPM are related phenomenologically by a linewidth enhancement factor α_H, also called Henry factor (Henry, 1982). The α_H-factor is defined as the ratio between the changes of the gain and the refractive index. In most publications (Henry, 1982; Agrawal & Olsson, 1989; Mecozzi & Mørk, 1997), the α_H-factor is assumed to be constant. This simplification indeed is valid only over a limited spectral range and for sufficiently small carrier density modulations in the SOA. Unfortunately, in most of the all-optical experiments, material properties change considerably and the α_H-factor varies significantly. In a new work (Wang et al., 2007), the temporal dynamics of the α_H-factor is investigated and it is shown that the α_H-factor changes during pump-probe experiments by more than an order of magnitude to the extent that even negative α_H-factors are observed.

After the control signal has died out, carriers recover. The carrier recovery process includes inter- and intraband carrier dynamics. The interband carrier dynamics limits the operation speed of the SOA. Especially, when subsequent control pulses are launched into a slow SOA (with a large carrier recovery time), the carrier density is progressively reduced. It recovers back to different levels and the amplifier gain also varies for different pulses, depending on the bit pattern seen by the SOA. This effect is usually called "pattern effect". The pattern effect is discussed with the help of the simulation and experiment in next section. The

numerical model used in the simulation was given in (Wang et al., 2007), while the parameters were adapted for the current SOA and validated experimentally.

2.3 Pattern effect in SOA based wavelength conversion

The XGM experiment conditions have a great influence on the gain and phase dynamics. The gain and phase dynamics are practically characterized by a carrier recovery time. A large carrier recovery time of an SOA means that the SOA response is slow. In a XGM, a very slow SOA shows a pattern effect, which is a serious problem in high-speed all-optical communications.

As subsequent control pulses are launched into a slow SOA, the carrier density is depleted continually. It recovers back to different levels and the amplifier gain also varies for different pulses, depending on the former bit pattern seen by the SOA. In our XGM experiment and simulation, 160 Gbit/s control signals with different bit patterns were launched into an SOA with a length of 1.6 mm. The output powers and phase shifts are compared in Fig. 4(a) for a bit pattern "1111000000000000", and in Fig. 4(b) for a bit pattern "1011010000000000".

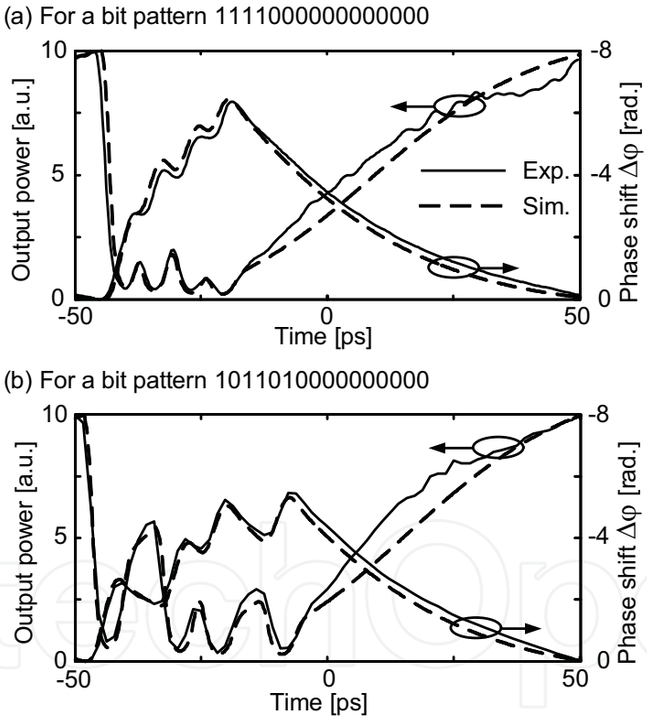

Fig. 4. Results of cross-gain modulation experiment with a bit pattern (a) 1111000000000000, and (b) 1011010000000000. Output power (left axis) and phase relaxation (right axis) are compared between experiment (solid lines) and simulation (dashed lines).

We see that the pattern effect will be a serious problem in high-speed signal processing. As shown in Fig. 4(a), the phase shift of subsequent bits increases but the relative phase shift between two subsequent bits is different. Sometimes, the pattern effect can be so strong that one bit "0" can not be recognized from bit "1"s, e.g. bit "0" in the bit pattern "1101" in Fig. 4(b).

Reducing pattern effect in an SOA can make SOA-based all-optical processing schemes working at high speed. Throughout this work, rather than decreasing the SOA recovery time by proper material design (Zhang et al., 2006) or choice of new fast materials (Sugawara et al., 2002), the main attention will be paid to mitigate pattern effect by optimum operation conditions and careful configuration design.

3. Pattern effect mitigation using an optical filter

3.1 SOA based wavelength conversion assisted by an optical filter

Recently, a new approach of a wavelength converter with an SOA followed by an optical filter was introduced and discussed, Fig. 5. For all-optical wavelength conversion, the input data signal P_{in} and the probe (cw) light P_{cnv} are launched into the SOA. In the SOA, the input data signal encodes the signal information by means of cross-gain and cross-phase modulations onto the cw signal. As a result, we obtain after the SOA an inverted signal P_{inv} at the wavelength of the cw light. The purpose of the subsequent passive optical filter with an appropriate amplitude and phase response is to reformat the signal P_{inv} into a new output-signal P_{cv} with a predetermined shape.

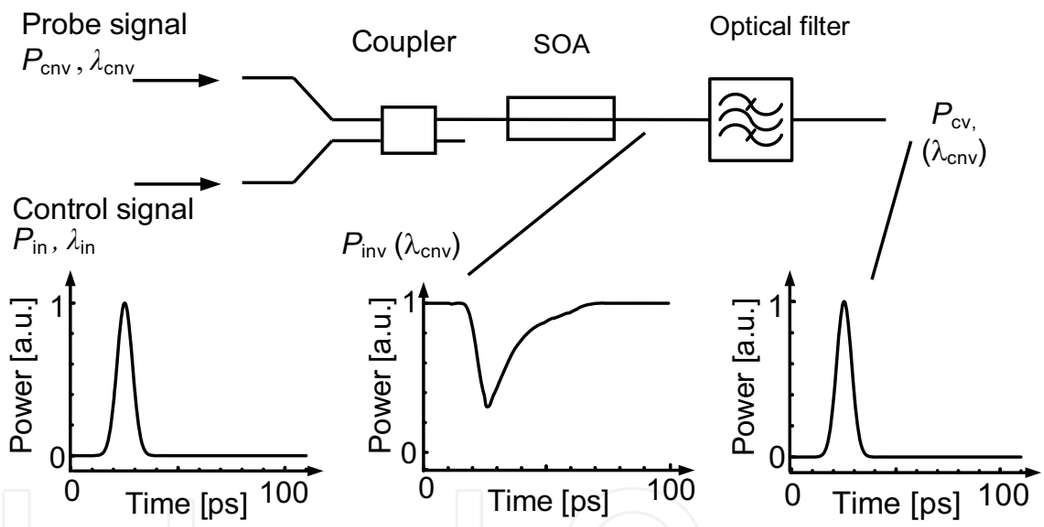

Fig. 5. All-optical wavelength converter based on an SOA followed by an optical filter.

Several filters have been proposed. These are the pulse-reformatting optical filter (PROF) (Leuthold et al., 2004a), the red-shift optical filter (RSOF) (Leuthold et al., 2003), the blue-shift optical filter (BSOF) (Leuthold et al., 2003; Nielsen et al., 2003; Liu et al., 2007), and a delay interferometer (DI) filter scheme (Leuthold et al., 2000; Leuthold et al., 2004b).

The PROF scheme can be understood as follows. As seen in Fig. 5 the probe signal P_{cnv} is cross-phase modulated by the control signal P_{in}, the P_{inv} signal after the SOA comprises a leading red-chirped (negative frequency variation with respect to time) component followed by a trailing blue-chirped (negative frequency variation with respect to time) component due to SOA carrier recovery. The P_{inv} signal also has a cw tone from the P_{cnv} signal. The PROF suppresses the cw tone and splits off the red and blue-chirped spectral components, which are subsequently recombined. This leads to a beating between the two signals that results in a strong and narrow converted pulse if the temporal delay between the two pulses

is adapted correctly. A schematic of the filter is depicted in Fig. 6(a) and the passband of the filter around the cw frequency f_{cw} is shown in the right part of Fig. 6(a).

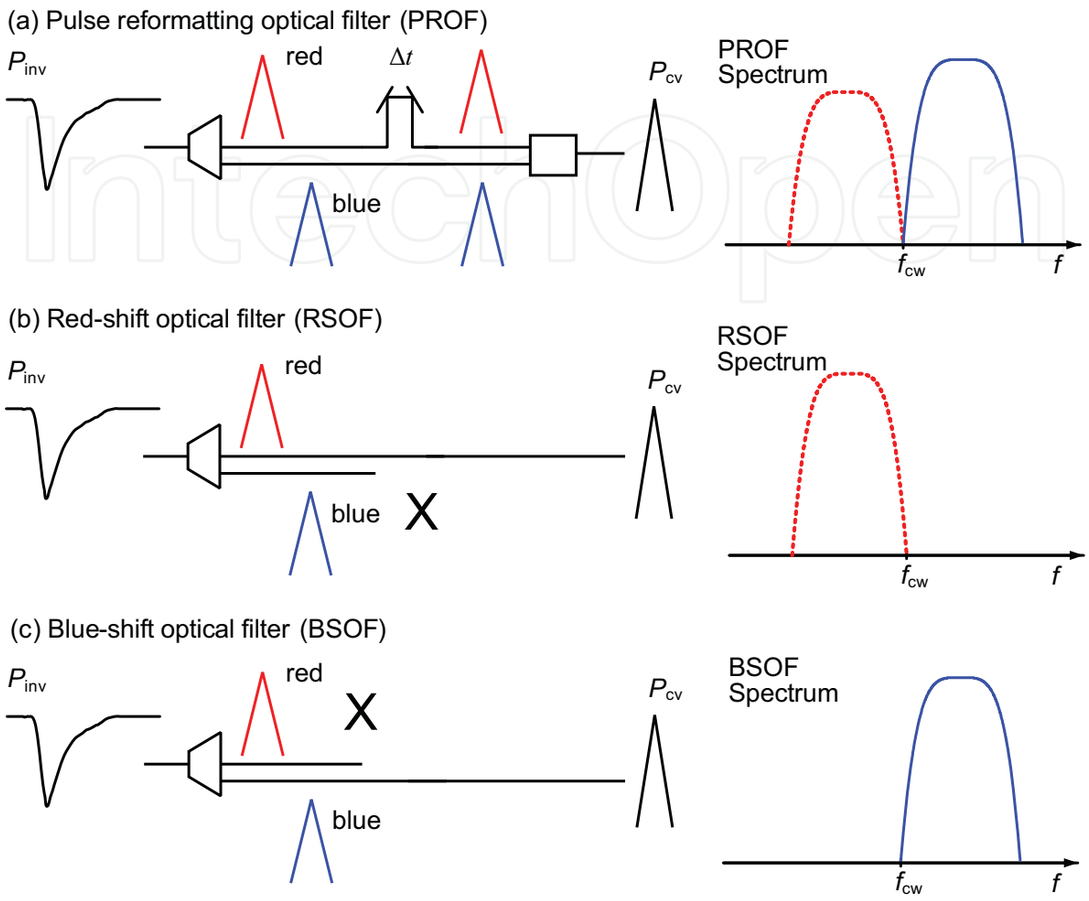

Fig. 6. Three different optical filter concepts for performing wavelength conversion. In the PROF scheme (a), the red- and blue-chirped spectral components are selected and combined with a proper temporal delay Δt between two paths. In the RSOF scheme (b), the red-chirped spectral component is selected and the blue-chirped spectral component is blocked (indicated with a symbol "X"). In the BSOF scheme (c), the blue-chirped spectral component is selected and the red-chirped spectral component is blocked.

The RSOF and BSOF schemes are similar to the PROF scheme, as shown in Fig. 6(b) and (c). Yet, either the red-chirped or the blue-chirped spectral components from the converted signals are selected by the respective filter, while the blue-chirped or the red-chirped spectral components are blocked as indicated by a symbol "X" in Fig. 6(b) and (c). With a proper choice of the BSOF's or RSOF's shape, the output signal P_{cv} shows a predetermined pulse shape.

The PROF, RSOF, and BSOF schemes exploit the fast chirp effects in the converted signal after the SOA, and are successful in performing high-speed wavelength conversion. However, so far it is not clear, if these schemes with optical filters can successfully overcome pattern effects at highest speed. In next section, we will investigate how to mitigate the pattern effect by using optical filters.

3.2 Pattern effect mitigation using a pulse reformatting optical filter

The scheme for the all-optical wavelength conversion with simultaneous pattern effect mitigation is shown in Fig. 7. The setup comprises an SOA followed by a pulse reformatting optical filter (PROF). The current PROF is built with discrete components, so that any parameters can be detuned and optimized individually. The PROF consists of a blue shifted optical filter (BSOF) and a red shifted optical filter (RSOF). An optical delay (OD) and a variable optical attenuator (VOA) were added after the RSOF. A conventional band-pass filter (BPF) has been added at the output of the PROF to curtail the spectrum of the converted signal to the ITU channel passband.

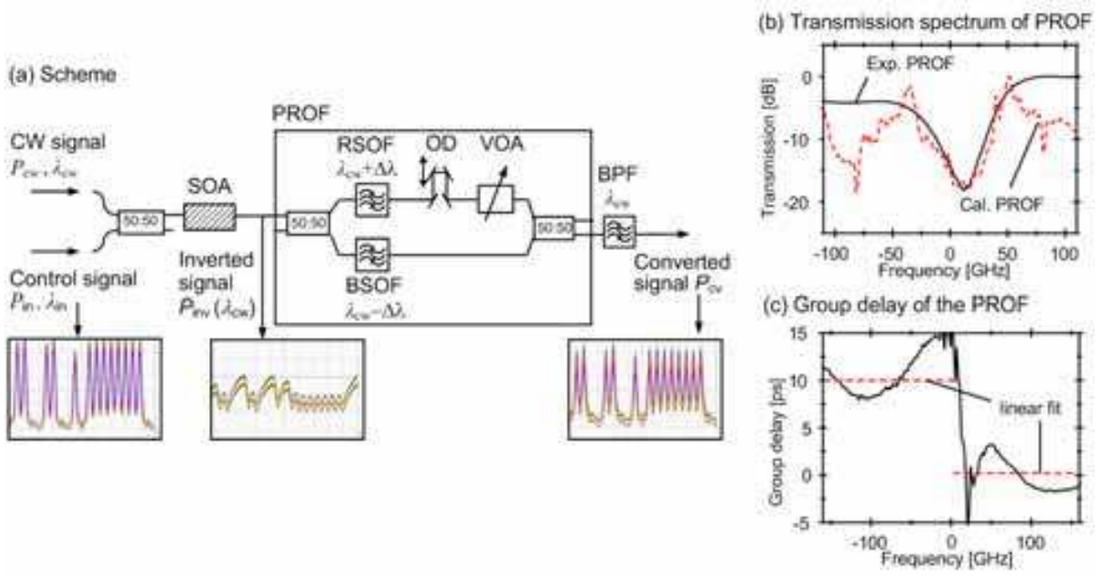

Fig. 7. (a) Wavelength conversion scheme with an SOA followed by a pulse reformatting optical filter (PROF), which transfers an inverted signal with strong pattern effect to non-inverted and pattern dependency removed signal. OD: optical delay, VOA: variable optical attenuator. (b) Transmission spectrum of PROF (dashed lines: calculated; solid line: as used in experiment). (c) Group delay of the PROF used in experiment. The dashed line is obtained from linear fitting.

The wavelength conversion with simultaneous pattern effect mitigation works as follows. A data signal modulates both the gain and the refractive index of the SOA thereby impressing the information in an inverted manner onto another continuous wave (cw) signal. Fig. 8(a) shows the pattern and power spectrum of the inverted cw signal behind the SOA. The leading edges of the converted light pulses are spectrally red-shifted (RS) whereas the trailing edges are blue-shifted (BS). In our scheme, we now split off the RS and the BS spectral components. The respective pattern and spectra are depicted in Fig. 8(b) and (c). The signal qualities of the respective signals are 13.0 dB and 7.9 dB. It can be noticed that the two signals have complimentary pattern effects. While the RS pattern shows an overshoot in the first bit in a sequence of '1's, the BS pattern undershoots particularly the first bit in a long sequence of '1's. When the two signals are combined – after introducing a proper delay and attenuation onto the RS signal – the two complimentary patterns compensate to each other, resulting in a non-inverted signal with a signal quality of as much as 17.8 dB. The pattern, eye diagram and the spectrum of the combined, wavelength converted signal are shown in Fig. 8(d).

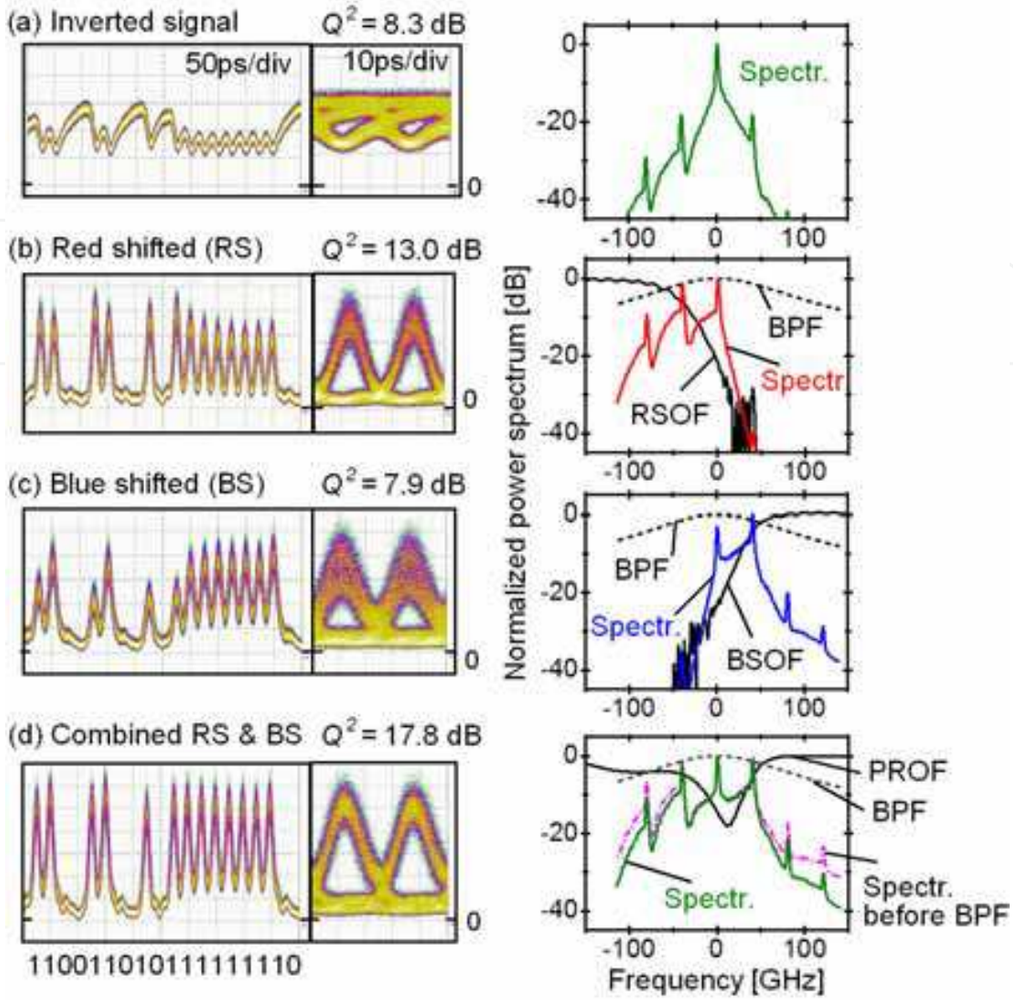

Fig. 8. Wavelength conversion experiment results, bit pattern (left column), eye diagram (middle column) and spectra with the filter shape (right column). Spectra are centred at the cw carrier frequency f_{cw}. (a) Inverted converted signal after the SOA, (c)–(d) RS, BS and combined signal.

In the experiment, a 33% RZ data signal at a bit rate of 40 Gbit/s with an average power P_{data} between –4 and 12.7 dBm and a carrier wavelength λ_{data} = 1530 nm was launched into the SOA. The pseudo-random data with a sequence length of 2^{11} –1 had a quality factor Q^2 = 19.8 dB. A cw signal with P_{cw} between –4 and 16 dBm and λ_{cw} = 1536.1 nm was coupled into the SOA. It became the wavelength converted signal. The bulk SOA of length L = 2.6 mm was biased at I = 750 mA. The non-saturated and saturated gain was 23 and 3 dB. The SOA recovery time (10% to 90%) was ~ 45 ps and polarization sensitivity was 0.5 dB. The plots in Fig. 8 have been recorded with a signal input power of 12.7 dBm and a cw power of 16 dBm. For this experiment we used two thin-film optical filters to realize the PROF. The parameters of the detuned filters are given in Table 1,

The optimum mode beating between red- and blue-chirped signals is obtained when two signals have similar amplitudes and the time delay between the red- and blue chirp vanishes (Leuthold et al., 2004). In our case we attenuated and delayed the red-chirped

Filter	Center λ [nm]	0.5 dB bandwidth [nm]	30 dB bandwidth [nm]	PMD [ps]
RSOF	1536.683	1.002	2.121	$\leq$ 0.10
BSOF	1535.352	1.035	2.148	$\leq$ 0.10

Table 1. Parameters of filters used. PMD: polarization mode dispersion.

signals by ~5 dB and 10 ps with respect to the blue-chirped signal. The transfer function of the optimized PROF has been measured. In Fig. 7(b) and (c), the transmission spectrum and group delay spectrum are depicted as solid lines. The ideal PROF filter transmission spectrum as derived from a calculation is plotted into the same figure (dashed lines). The PROF filter used in the experiment and the ideal filter are fairly similar. The Q^2-factors reported in Fig. 8 were recorded for the best combined signal. In our case, by varying the position of the filters, the Q^2-factor of the BS signal could be as good as 9.9 dB, while the Q^2-factor of the RS signal could not be improved beyond the 13 dB reported above.

The PROF scheme uses both the red- and blue-shifted spectral components, thus keeps all the information in the spectrum. This advantage leads a to a large input power dynamic range, in which a good signal quality is kept. In our experiments, we obtained a Q^2-factor of 15.8 dB with an input power (λ_{in} = 1530 nm) of as low as –4.3 dBm while a cw power (λ_{cw} = 1536.1 nm) is –4 dBm. At an input data power of 12.9 dBm, which is the available maximum in our experiment, and a cw power of 14.7 dBm, we also got a Q^2-factor of 18.2 dB. In fact, throughout this input power dynamic range of at least 17.2 dB with an adjustment of the cw power, we always got Q^2-factors above 15.6 dB, shown in Fig. 9. Note that the cw power adjustment for respective input data powers was stopped as long as we have a Q^2-factor above 15.6 dB. All of Q^2 values were measured with a bit-error rate test (BERT) and then interpolated from the inverse complementary error function. Yet, as it is not clear on what noise distribution we have after an all-optical wavelength conversion operation. The Q^2 values may differ based on the method used. However, the quantitative values given here are still indicative for the quality of the signal.

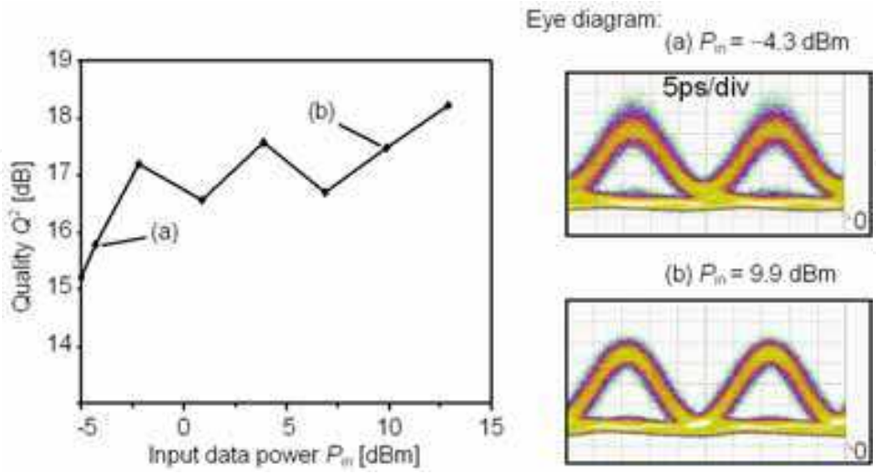

Fig. 9. Signal qualities of the converted signal for various input data powers without adaptation of filter parameters but with adaptation of the cw input power levels, while λ_{in} = 1530 nm and λ_{cw} = 1536.1 nm. Eye diagram for P_{in} = –4.3 dBm and 9.9 dBm are given in (a) and (b) respectively.

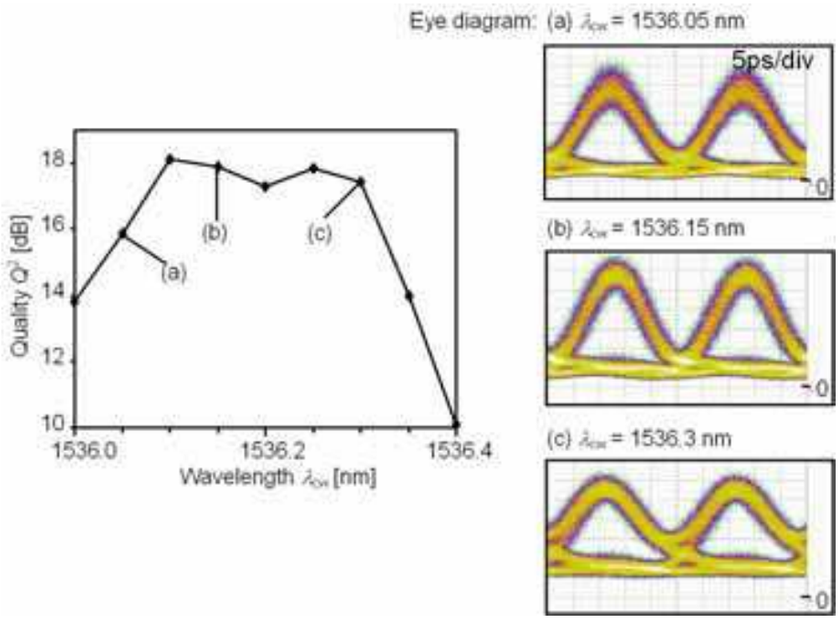

Fig. 10. Signal qualities of the converted signal for various cw wavelengths without adaptation of filter parameters, while the cw power P_{cw} = 14.7 dBm and the input power P_{in} = 12.9 dBm at λ_{in} = 1530 nm. Eye diagrams for λ_{cw} = 1536.05 dBm, 1536.15 dBm and 1536.3 nm are given in (a), (b) and (c) respectively.

Except a large input power dynamic range, the PROF scheme features a large tolerance of the operating wavelength. In the experiment, we kept the input power P_{in} = 12.9 dBm at λ_{in} = 1530 nm and the cw power P_{cw} = 14.7 dBm, while the operating wavelength of the cw signal λ_{cw} varied from 1536.0 nm to 1536.4 nm. The measured Q^2-factor is depicted in left part of Fig. 10. We see that a wavelength tolerance for a Q^2–factor above 15.6 dB is about 0.29 nm. Eye diagram for λ_{cw} = 1536.05 nm, 1536.15 nm and 1536.3 nm are given in Fig. 10(a), (b) and (c) respectively. All the eyes are clean and open.

3.3 Complementary pattern effects in the XPM-induced chirp

Now we investigate the complementary pattern effects in the XPM-induced red and blue chirp of the inverted signal. The complementary pattern effects have their origin in the carrier dynamics of the SOA. We therefore used an SOA model from (Wang et al., 2007) that encompasses both slow and fast carrier recovery effects. The parameters in (Wang et al., 2007) were adapted for the current SOA and validated experimentally. Two second-order Gaussian filters with a 3dB bandwidth of 120 GHz were used as the RSOF and the BSOF in the simulation to select the spectral components. Simulation results are given in Fig. 11. An exemplary input data signal with a bit pattern "0111", Fig. 11(a), is launched into the SOA. Fig. 11(b) shows the gain evolution with time. The gain decreases with the leading edge of each input pulse and recovers with the falling edge of each pulse. Further, with each sub-sequent bit the SOA gain gradually saturates. Due to Kramers-Kronig relation, a gain change is always accompanied by a phase-shift $\Delta\varphi_{NL}$, whose variation per time increment Δt in consequence determines the instantaneous frequency shift Δf (i.e. chirp, see formula of Fig. 11(c)). The leading edges of the input pulses induce a red chirp, while the trailing edges induce a blue chirp, Fig. 11(c). As we will see below, these two chirps have different pattern dependences.

We first study the pattern dependence of the signal after the RSOF. The first "1" bit in the pulse train induces strong carrier depletion and a large gain reduction Fig. 11(b). A strong carrier-depletion induces a large phase-shift and consequently a large red chirp on the leading edge, Fig. 11(c). For subsequent "1" pulses, the SOA does not fully recover. The gain for subsequent "1" pulses is smaller than for the first "1" bit. Therefore the carrier depletion decreases. As the gain reduction due to the carrier depletion decreases, the induced red chirp decreases as well, low part of Fig. 11(c). This decreasing red chirp however, by means of the RSOF filter transfer function (see 1,2,3 in Fig. 11(d)), and the increasing gain saturation create a bit pattern with decreasing power level, shown in Fig. 11(e) bottom.

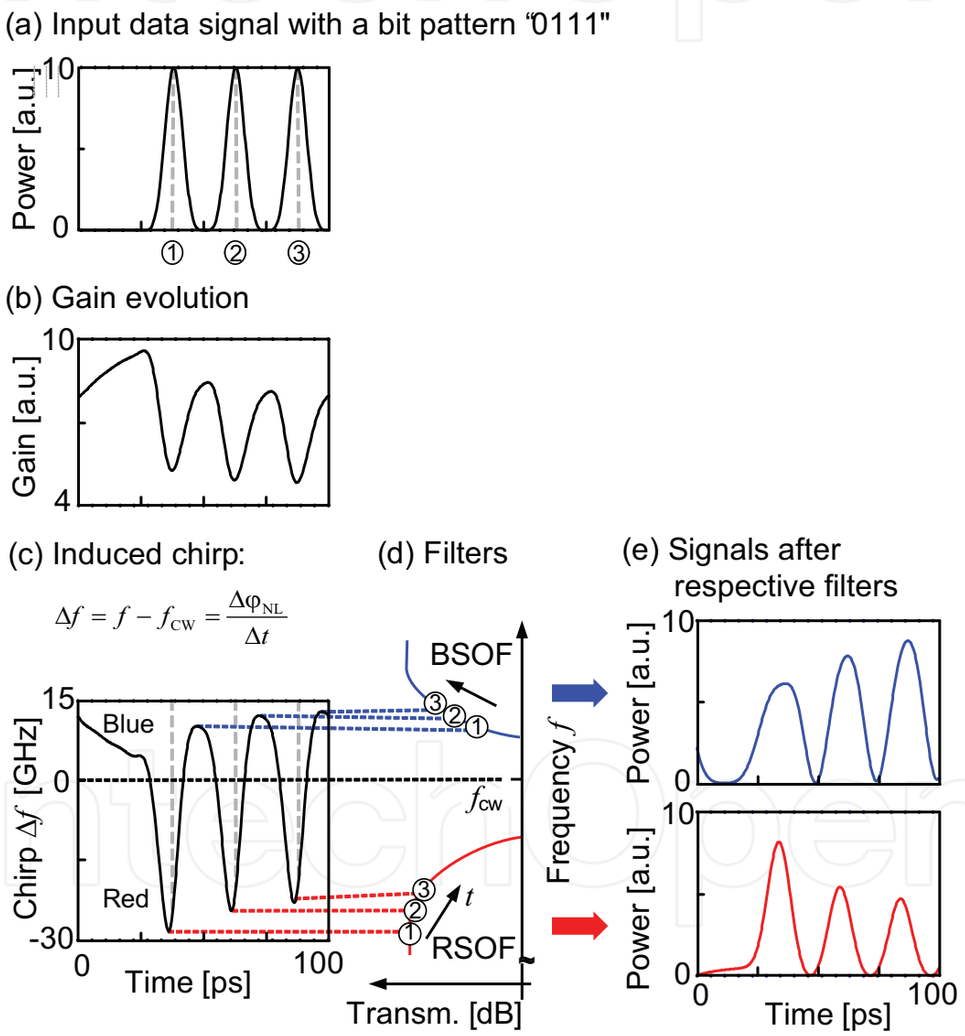

Fig. 11. Complementary pattern effects by frequency-amplitude conversion through differently centred filters. (a) Input data pulse train. (b) Simulated gain evolution in SOA and (c) induced frequency chirp in the inverted signal. (d) Schematic filter shape of the BSOF and the RSOF. (e) Pattern dependence in blue and red-spectral components after sending signal (b) with chirp (c) through filter plotted in (d). Dashed lines in (a), (b) and (c) indicate the time positions of the input three pulses.

The bit pattern of the signal behind the BSOF can be understood as follows. The gain recovers with the trailing edge of the first "1" pulse, creating a blue chirp. With subsequent bits launched into the SOA, the SOA is further saturated and the overall gain G decreases with following "1" bits. In turn the carrier depletion due to stimulated emission is now weaker while the current injection is unchanged. As a consequence, the carrier recovery rate is faster for subsequent pulses. This leads to a stronger blue-chirp as also observed in the simulation depicted in Fig. 11(c). By positioning the strongest blue-chirped signals closest to the centre of the BSOF passband, Fig. 11(d), transmission of the strongest chirped pulse is favoured. This leads to an increasing power level for the tails of longer patterns, shown in Fig. 11(e) top. The coherent superposition of the red- and blue-shifted signal with opposite patterns then leads to the pattern effect compensated output, Fig. 11(d). The scheme works well, as long as the frequency-amplitude conversion at the slope of the BSOF can over-compensate the gain saturation. Simulations show that results do not change for a 3 dB filter bandwidth of 80 to 220 GHz.

7. Conclusion

In this work, we investigate an SOA-based all-optical wavelength conversion scheme with an assisting optical filter after the SOA. The technique utilizes the complementary pattern effects of the XPM induced red and blue chirp in SOAs. By carefully selecting the optical filters and compensating the complementary pattern effects in the red and blue chirp to each other, a pattern effect mitigated converted signal is obtained. These advantages lead to a larger operation wavelength tolerance and a large input power dynamic range, in which a good signal quality is kept. This scheme is experimentally demonstrated having a ~0.3 nm operation wavelength range and over 17 dB input power dynamic range. This concept has been demonstrated at 40 Gbit/s, however, the general principle holds for higher speed.

8. References

Agrawal G. P. & Olsson N. A. (1989). Self-phase modulation and spectral broadening of optical pulses in semiconductor laser amplifiers. *IEEE J Quantum Electron.*, Vol. 25, No. 11, p2297-2306, 1989.

Bischoff S.; Nielsen M. L. & Mørk J. (2004). Improving the all-optical response of SOAs using a modulated holding signal. *IEEE J Lightw. Technol.*, Vol. 22, No. 5, 1303-1308, 2004.

Connelly M. J. (2002). *Semiconductor Optical Amplifiers*, Springer-Verlag, Boston, MA, 2002.

Durhuus, T.; Mikkelsen, B.; Joergensen, C.; Lykke Danielsen, S.; Stubkjaer, K.E. (1996). All optical wavelength conversion by semiconductor optical amplifiers. *IEEE J Lightw. Technol.*, Vol. 14, No. 6, 942–954, 1996.

Eiselt, M.; Pieper, W.; Weber, H.G. (1995). SLALOM: Semiconductor laser amplifier in a loop mirror. *IEEE J Lightw. Technol.*, Vol. 13, No. 10, 2099-2112, 1995.

Girardin, F. ; Guekos, G. ; Houbavlis, A. (1998). Gain recovery of bulk semiconductor optical amplifiers. *IEEE Photon. Technol. Lett.*, Vol. 10, No. 6, 784-786, 1998.

Hall K. L. & Rauschenbach K. A. (1998). 100-Gb/s bitwise logic. *Opt. Lett.*, Vol. 23, No. 8, 1271–1273, 1998.

Henry C. H. (1982). Theory of the linewidth of semiconductor lasers. *IEEE, J Quantum Electron.*, Vol. QE-18, No. 2, 259-264, 1982.

Kumar, S. ; Zhang, B. ; Willner, A.E. (2006). Elimination of data pattern dependence in SOA-based differential-mode wavelength converters using optically-induced birefringence. *Proceedings of Optical Fiber Communication Conference*, 3 pp., Anaheim, California, USA, March 2006, IEEE Computer Society Press, Washington.

Leuthold, J. ; Joyner, C.H. ; Mikkelsen, B. ; Raybon, G. ; Pleumeekers, J.L. ; Miller, B.I. ; Dreyer, K. ; Burrus, C.A. (2000). 100-Gb/s all-optical wavelength conversion with integrated SOA delayed-interference configuration. *Electron. Lett.*, Vol. 36, No. 13, 1129-1130, 2000.

Leuthold, J. ; Ryf, R. ; Maywar, D.N. ; Cabot, S. ; Jaques, J. ; Patel, S.S. (2003). Nonblocking all-optical cross connect based on regenerative all-optical wavelength converter in a transparent network demonstration over 42 nodes and 16800 km. *J Lightw. Technol.*, Vol. 21, No. 11, 2863-2870, 2003.

Leuthold, J. ; Marom, D.M. ; Cabot, S. ; Jaques, J.J. ; Ryf, R. ; Giles, C.R. (2004a) All-optical wavelength conversion using a pulse reformatting optical filter. *IEEE J Lightw. Technol.*, Vol. 22, No. 1, 186-192, 2004.

Leuthold, J.; Moller, L. Jaques, J. Cabot, S. Zhang, L. Bernasconi, P. Cappuzzo, M. Gomez, L. Laskowski, E. Chen, E. Wong-Foy, A. Griffin, A. (2004b). 160 Gbit/s SOA all-optical wavelength converter and assessment of its regenerative properties. *Electron. Lett.*, Vol. 40, No. 9, 554-555, 2004.

Liu, Y.; Tangdiongga, E.; Li, Z.; de Waardt, H.; Koonen, A.M.J.; Khoe, G.D.; Shu X.; Bennion, I.; Dorren, H.J.S. (2007). Error-free 320-Gb/s all-optical wavelength conversion using a single semiconductor optical amplifier. *IEEE J Lightw. Technol.*, Vol. 25, No. 1, 103-108, 2007.

Manning R. J. & Davies D. A. O. (1994). Three-wavelength device for all-optical signal processing. *Opt. Lett.*, Vol. 19, No. 12, 889-891, 1994.

Manning, R.J.; Yang, X.; Webb, R.P.; Giller, R.; Garcia Gunning, F.C.; Ellis, A.D. (2006). The 'turbo-switch' – a novel technique to increase the high-speed response of SOAs for wavelength conversion. *Proceedings of Optical Fiber Communication Conference*, 3 pp., Anaheim, California, USA, March 2006, IEEE Computer Society Press, Washington.

Nielsen M.; Lavigne B.; Dagens B. (2003). Polarity-preserving SOA-based wavelength conversion at 40 Gbit/s using bandpass filtering. *IEEE Electron. Lett.*, Vol. 39, No. 18, 1334-1335, 2003.

Nielsen M. & Mørk J. (2006). Bandwidth enhancement of SOA-based switches using optical filtering: theory and experimental verification. *Opt. Express*, Vol. 14, No. 3, 1260-1265, 2006.

Saitoh T. & Mukai T. (1989). Structural design for polarization-insensitive travelling-wave semiconductor laser amplifiers. *Opt. and Quantum Electron.*, Vol. 21, No. 1, s47-s58, 1989.

Sugawara M.; Akiyama T.; Hatori N.; Nakata Y.; Ebe H. & Ishikawa H. (2002). Quantum-dot semiconductor optical amplifiers for high-bit-rate signal processing up to 160 Gb/s and a new scheme of 3R regenerators. *Meas. Sci. Technol.*, Vol. 13, No. 11, 1683-1691, 2002.

Tajima K. (1993). All-optical switch with switch-off time unrestricted by carrier lifetime. *Jpn. J Appl. Phys.*, Vol. 32, No. 12A, L1746-L1749, 1993.

Wang J.; Maitra, A.; Poulton, C.G.; Freude, W.; Leuthold, J. (2007). Temporal dynamics of the alpha factor in semiconductor optical amplifiers. *IEEE J Lightw. Technol.*, Vol. 25, No. 3, 891-900, 2007.

Yoo, S. J. B. (1996). Wavelength conversion technologies for WDM network applications. *IEEE J Lightw. Technol.*, Vol. 14, No. 6, 955-966, 1996.

Zhang, L.; Kang, I.; Bhardwaj, A.; Sauer, N.; Cabot, S.; Jaques, J.; Neilson, D.T. (2006). Reduced recovery time semiconductor optical amplifier using p-type-doped multiple quantum wells. *IEEE Photon. Technol. Lett.*, Vol. 18, No. 22, 2323-2325, 2006.

IntechOpen

IntechOpen

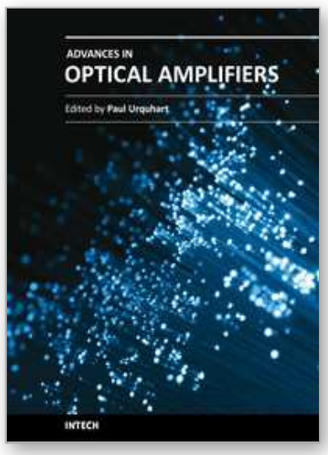

Advances in Optical Amplifiers
Edited by Prof. Paul Urquhart

ISBN 978-953-307-186-2
Hard cover, 436 pages
Publisher InTech
Published online 14, February, 2011
Published in print edition February, 2011

Optical amplifiers play a central role in all categories of fibre communications systems and networks. By compensating for the losses exerted by the transmission medium and the components through which the signals pass, they reduce the need for expensive and slow optical-electrical-optical conversion. The photonic gain media, which are normally based on glass- or semiconductor-based waveguides, can amplify many high speed wavelength division multiplexed channels simultaneously. Recent research has also concentrated on wavelength conversion, switching, demultiplexing in the time domain and other enhanced functions. Advances in Optical Amplifiers presents up to date results on amplifier performance, along with explanations of their relevance, from leading researchers in the field. Its chapters cover amplifiers based on rare earth doped fibres and waveguides, stimulated Raman scattering, nonlinear parametric processes and semiconductor media. Wavelength conversion and other enhanced signal processing functions are also considered in depth. This book is targeted at research, development and design engineers from teams in manufacturing industry, academia and telecommunications service operators.

How to reference
In order to correctly reference this scholarly work, feel free to copy and paste the following:

Jin Wang (2011). Pattern Effect Mitigation Technique Using Optical Filters for Semiconductor-Optical-Amplifier Based Wavelength Conversion, Advances in Optical Amplifiers, Prof. Paul Urquhart (Ed.), ISBN: 978-953-307-186-2, InTech, Available from: http://www.intechopen.com/books/advances-in-optical-amplifiers/pattern-effect-mitigation-technique-using-optical-filters-for-semiconductor-optical-amplifier-based-

INTECH
open science | open minds

InTech Europe
University Campus STeP Ri
Slavka Krautzeka 83/A
51000 Rijeka, Croatia
Phone: +385 (51) 770 447
Fax: +385 (51) 686 166
www.intechopen.com

InTech China
Unit 405, Office Block, Hotel Equatorial Shanghai
No.65, Yan An Road (West), Shanghai, 200040, China
中国上海市延安西路65号上海国际贵都大饭店办公楼405单元
Phone: +86-21-62489820
Fax: +86-21-62489821

© 2011 The Author(s). Licensee IntechOpen. This chapter is distributed under the terms of the Creative Commons Attribution-NonCommercial-ShareAlike-3.0 License, which permits use, distribution and reproduction for non-commercial purposes, provided the original is properly cited and derivative works building on this content are distributed under the same license.

IntechOpen

IntechOpen